Mercury Stable Isotopes in Seabirds in the Ebro Delta (Ne Iberian Peninsula): Inter-Specific and Temporal Differences

Moisès Sánchez-Fortún, David Amouroux, Emmanuel Tessier, Josep Lluís Carrasco, Carola Sanpera

Mercury stable isotopes in seabirds in the Ebro Delta (NE Iberian Peninsula): inter-specific and temporal differences

Moisès Sánchez-Fortún[a,b]*, David Amouroux[c], Emmanuel Tessier[c], Josep Lluís Carrasco[d], Carola Sanpera[a,b]

Authors' affiliations:

a. Department of Evolutionary Biology, Ecology and Environmental Sciences, University of Barcelona, Barcelona, Spain

b. Institut de Recerca de la Biodiversitat (IRBio), University of Barcelona, Barcelona, Spain

c. Université de Pau et des Pays de l'Adour, E2S UPPA, CNRS, IPREM, Institut des Sciences Analytiques et de Physico-chimie pour l'Environnement et les matériaux, Pau, France

d. Biostatistics, Department of Basic Clinical Practice, University of Barcelona, Barcelona, Spain

Authors' email addresses: MSF (m.sanchezfortun.ub@gmail.com); ET (emmanuel.tessier@univ-pau.fr); DA (david.amouroux@univ-pau.fr); JLC (jlcarrasco@ub.edu); CS (csanpera@ub.edu)

***Corresponding author**: Moisès Sánchez-Fortún. Department of Evolutionary Biology, Ecology and Environmental Sciences, University of Barcelona, Barcelona, Spain and Institut de Recerca de la Biodiversitat (IRBio), University of Barcelona, Barcelona, Spain. m.sanchezfortun.ub@gmail.com

Keywords: **feathers, Laridae, anthropogenic mercury, Mediterranean, Audouin's gull**

Abstract

Mercury (Hg) is a global pollutant, which specially affects aquatic ecosystems, both marine and freshwater. Top-predators depending on these environments, such as seabirds, are regarded as suitable bioindicators of Hg pollution. In the Ebro Delta (NE Iberian Peninsula), legacy Hg pollution from a chlor-alkali industry operating in Flix and located ca. 100 km upstream of the Ebro River mouth has been impacting the delta environment and the neighboring coastal area. Furthermore, natural occurring levels of Hg in the Mediterranean Sea are known to be high compared to other marine areas. In this work we used a Hg stable isotopes approach in feathers to disentangle the Hg sources and processes leading to different Hg concentrations in three *Laridae* species breeding in sympatry in the area (Audouin's gull *Ichtyaethus audouinii*, black-headed gull *Chroicocephalus ridibundus*, common tern *Sterna hirundo*). These species have distinct trophic ecologies and make a different use of marine resources and rice paddies prey. Moreover, for Audouin's gull in which in the Ebro Delta colony temporal differences in Hg levels were documented previously, we investigated the change in the contribution of different Hg sources using the same approach. Hg stable isotopes differentiated the three different species according to their trophic ecologies. Furthermore, for Audouin's gull we observed temporal variations in Hg isotopic signatures possibly owing to anthropogenic-derived pollution in the Ebro Delta. To the best of our knowledge this is the first time Hg stable isotopes have been reported in seabirds from the NW Mediterranean.

1. Introduction

Mercury (Hg) is considered a global pollutant, which is present in all Earth compartments, and exerts detrimental effects on both humans and wildlife (Clarkson and Magos 2006; Discroll et al. 2013; Evers 2018). Although Hg naturally occurs in the environment, it can also be found as result of human activities (Discroll et al. 2013). Among anthropogenic activities introducing mercury into the environment are artisanal gold mining or industrial processes (e.g., coal combustion, chlor-alkali plants) (UNEP 2019). Anthropogenic activities have significantly increased mercury levels in the environment since the pre-industrial era (Amos et al. 2013; UNEP 2019), which poses an urge to monitor environmental loads of this pollutant and be able to distinguish between anthropogenic and natural sources in order to help environmental-related decisions (Wiener et al. 2003).

Particularities of this element include a complex biogeochemical cycle resulting in chemical speciation (Selin 2009; Gustin et al. 2020), which depends on both the biotic and abiotic factors in the environment where mercury is found (Ullrich et al. 2001; Lyman et al. 2020; Bowman et al. 2020). For instance, in aquatic environments, inorganic mercury (Hg^{2+}) is known to be methylated by mainly sulfate- and iron-reducing bacteria (Podar et al. 2015), but also by abiotic processes (Celo et al. 2006), transforming Hg^{2+} into methylmercury (MeHg). MeHg is a readily bioavailable and highly toxic form of mercury which can bioaccumulate in organisms and get biomagnified along food webs (Morel et al. 1998; Lavoie et al. 2013; Evers 2018).

In this context, top-predator and long-lived species, such as seabirds, are more exposed to Hg and its negative effects including physiological, reproductive, neurological and teratogenic effects (Whitney and Cristol 2017). In fact, seabirds have been extensively used as bioindicator species of environmental pollution for an array of contaminants, including mercury (Furness and Camphuysen 1997; Becker et al. 2002; Burger and Gochfeld 2004; Sanpera et al. 2007; Blévin et al. 2013; Albert et al. 2019; Bond and Lavers 2020).

The Ebro Delta (NE Iberian Peninsula) comprises 30 000 ha of wetlands, with 75% of its area used for rice-farming, 20% protected as a natural reserve, and 5% is urbanized (Mañosa et al. 2001). Since the late 19th century, a chlor-alkali plant has been operating ca. 100 km upstream the Ebro River mouth. During the active period of the plant, 550 000 – 700 000 m^3 of contaminated sediments, mainly with mercury and organochlorine compounds, were

accumulated on the bottom of the river dam, close to the factory (Grimalt et al. 2003; ACA 2013). Although the production of chlorine using mercury ceased in 2017, legacy mercury pollution persists and has been impacting all the environments in the Ebro River delta, because of the transport of contaminated particles along the river (Carrasco et al. 2010, 2011; Cotín et al. 2012; Campillo et al. 2019; Palanques et al. 2020). Moreover, during 2013-2014, a sediment remediation plan, including the dredging and disposal of polluted sediments, was implemented to remove toxicants from the riverbed in the vicinity of the factory. In a previous study, Sánchez-Fortún et al. (2020) reported the possible influence of the remediation tasks which took place in 2013-2014 on the increase of mercury levels observed in the Audouin's gull breeding colony in the Ebro Delta area. Furthermore, due to its biogeochemical characteristics and local Hg reservoirs, methylmercury levels in the Mediterranean Sea are high compared to other oceanic regions (Cossa and Coquery 2005). Thus, seabird species depending on food webs from the Ebro Delta area might be also exposed to naturally high levels of mercury (Arcos et al. 2002; Sanpera et al. 2007; Cotín et al. 2011; Sánchez-Fortún et al. 2020). However, the relative importance of mercury sources impacting aquatic habitats from the area (freshwater or coastal areas) has never been analyzed in depth.

In systems with acknowledged anthropogenic sources of Hg pollution, Hg stable isotopes have proven as an useful tool to unravel origins of Hg burdens in an array of environmental compartments (e.g., sediments [Gehrke et al. 2011; Wiederhold et al. 2015; Reinfelder and Janssen 2019], atmosphere [Estrade et al. 2010]), and in humans (Laffont et al. 2009; 2011) and wildlife (Day et al. 2012; Kwon et al. 2014; Bonsignore et al. 2015).

Mercury has seven stable isotopes with atomic masses 196, 198, 199, 200, 201, 202, and 204 amu, which can undergo both mass-dependent fractionation (MDF) and mass-independent fractionation (MIF). MDF occurs as consequence of physical, chemical and biological processes including mercury biological methylation and demethylation (Kritee et al. 2009; Rodríguez-González et al. 2009; Janssen et al. 2016), photoreduction (Bergquist and Blum 2007), trophic transfer (Laffont et al. 2009), metabolic reactions (Laffont et al. 2009; Feng et al. 2015; Renedo et al. 2020; 2021). MIF occurs mainly as consequence of photochemical reactions in the water column prior to bioaccumulation of Hg (Bergquist and Blum 2007). Although MIF processes have been described for isotopes ^{200}Hg and ^{204}Hg (i.e., even-MIF), and for ^{199}Hg and ^{201}Hg (i.e., odd-MIF; Kwon et al. 2020), odd-MIF has been observed commonly in biological samples (Tsui et al. 2020). Thus, MDF and MIF signatures offer a

framework to trace Hg pollution and may provide information on Hg sources in organisms. This information coupled with carbon and nitrogen stable isotopes values, which have been used extensively as proxies of the trophic ecology of organisms (Post 2002; Boecklen et al. 2011), might provide valuable information on the causes leading to high Hg levels in wildlife.

The main aim of this study is to relate the trophic ecology of different *Laridae* species inhabiting in the Ebro Delta area to the total-Hg (THg) burden found in the organism and potential Hg sources at local scale. We have analyzed Hg stable isotopes in feathers of fledgling individuals of three different species breeding in the Ebro Delta, that present contrasted dietary characteristics: the common tern (*Sterna hirundo*; SH), an epipelagic marine forager (Cotín et al. 2011), the black-headed gull (*Chroicocephalus ridibundus*; CR), which mostly forages in rice-fields (Antón-Tello et al. 2021), and the Audouin's gull (*Ichthyaetus audouinii;* IA), which forages in both marine environments (fisheries discards) and in rice-fields (Sanpera et al. 2007; García-Tarrasón et al. 2015). We then analyzed the stable isotopes of Hg to unravel the differential contribution of various Hg sources over years on the Audouin's gull breeding colony in the Ebro Delta, to comprehend if differences of this metal observed from before and after 2013, when the remediation plan was applied (Sánchez-Fortún et al. 2020), are related to changes in Hg sources.

2. Materials and methods

2.1. Fieldwork and sample collection

As part of a continued monitoring program of the Audouin's gull (*Ichthyaethus audouinii*, IA) breeding colony in the Ebro Delta (NE Iberian Peninsula: 40°33' N, 00°390' E), 10-15 mantle feathers of juvenile individuals (approx. 3 weeks old) were sampled on years 2010, 2013, 2014, 2017 (N = 10 individuals each year; see Sánchez-Fortún et al. 2020 for further details on sampling). Additionally, during the breeding season of 2017, 10-15 mantle feathers of juvenile individuals from the following species breeding in the Ebro Delta area were sampled (N = 10 individuals for each species): common tern (*Sterna hirundo,* SH; approx. 3 weeks old), black-headed gull (*Chroicocephalus ridibundus*, CR; approx. 3 weeks old). Feathers were stored in zip-lock bags until analysis.

2.2. Total mercury determination

Total mercury (THg) determination in our samples was performed at the Scientific and Technological Centers of the University of Barcelona (Spain). Feather samples were washed using 0.25 M NaOH and rinsed with distilled water to remove external Hg contamination (Bearhop et al. 2000). After cleaning, samples were oven dried to constant mass at 50°C and then ground to a homogenous powder with an impactor mill (Freezer Mill 6850, SpexCertiPrepH Inc., Metuchen, NJ, USA) operating at liquid nitrogen temperature. THg in feathers (ng/g dry weight) was determined by combustion using a Direct Mercury Analyzer (Milestone® DMA-80) for all the species samples from 2017, or by Induction Coupled Plasma-Mass Spectrometer (ICP-MS) for Audouin's gull samples from 2010, 2013 and 2014. DMA-80 analyses were directly analyzed by combustion using 0.20-0.30 mg of feather sample. For the ICP-MS mercury determinations, ~30 mg of feather sample were acid digested in a microwave oven using 1-2 mL of nitric acid (HNO_3 70%) and 0.5-1 mL of hydrogen peroxide (H_2O_2 30%) in Teflon containers. To check for the accuracy of measurements for both methods, we analyzed a certified reference material in duplicate (NIES-13 Human Hair CRM) every 10 to 15 samples with recoveries ranging from 91% to 94% for DMA-80 analyses and 97 to 103% in ICP-MS analyses. Thus, no corrections were applied to the THg values of the samples prior to statistical analyses.

2.3. Analysis of mercury stable isotopes

Stable isotopes of mercury were analyzed following method and protocol reported by Renedo et al. (2018). Aprox. 0.2 g of feather powder was digested with 5 mL of HNO_3 (65%, INSTRA quality) and 1/3 of the total volume of H_2O_2 (30%, ULTREX quality), and extracted in Hotblock at 75 °C during 8h (6h in HNO_3, plus 2h after the addition of H_2O_2). Hg isotopic composition for each of the 6 most abundant stable isotopes of Hg (^{198}Hg, ^{199}Hg, ^{200}Hg, ^{201}Hg, ^{202}Hg and ^{204}Hg) was determined by means of a cold-vapor generator (CVG)-multicollector (MC)-ICPMS (Nu Instruments). Hg isotopic values were reported using the delta notation relative to the bracketing standard NIST-3133 certified reference material. Instrumental mass-bias was corrected using the internal Tl standard, NIST 997 CRM. A secondary standard NIST RM-8160 (UM-Almadén standard) was used for validation of the analytical session. Furthermore, NIES-13 Human Hair CRM and an internal reference material composed of king penguin feathers (F-KP) were used for the Hg stable isotopes analyses. Results on mercury

stable isotopes analyses are reported in detail in Table S1, Table S2 and Table S3 from the Supplementary Materials.

Mass-dependent fractionation (MDF) is reported as δ^{202}Hg values (‰) calculated as follows (Blum and Bergquist 2007):

$$\delta^{202}\text{Hg} = [(^{202}\text{Hg}/^{198}\text{Hg})_{\text{sample}}/(^{202}\text{Hg}/^{198}\text{Hg})_{\text{NIST3133}} - 1] \times 1000$$

Mass-independent Hg isotopic fractionation (MIF) is reported as Δ^{199}Hg, Δ^{200}Hg, Δ^{201}Hg, Δ^{204}Hg (‰), calculated using the difference by the δ^{xxx}Hg value and a value predicted based on MDF (Bergquist and Blum 2007):

$$\Delta^{204}\text{Hg} \approx \delta^{204}\text{Hg} - (\delta^{202}\text{Hg} \times 1.493)$$
$$\Delta^{201}\text{Hg} \approx \delta^{201}\text{Hg} - (\delta^{202}\text{Hg} \times 0.752)$$
$$\Delta^{200}\text{Hg} \approx \delta^{200}\text{Hg} - (\delta^{202}\text{Hg} \times 0.502)$$
$$\Delta^{199}\text{Hg} \approx \delta^{199}\text{Hg} - (\delta^{202}\text{Hg} \times 0.252)$$

Where Δ^{199}Hg and Δ^{201}Hg are known as odd-MIF, and Δ^{200}Hg and Δ^{204}Hg as even-MIF. Additionally, we calculated the ratio $\Delta^{199}\text{Hg}/\Delta^{201}\text{Hg}$, which has proven to be indicative of different photochemical transformation processes and speciation of Hg (i.e., photoreduction of Hg(II) *vs*. photodemethylation of MeHg) in experimental settings (Bergquist and Blum 2007). $\Delta^{199}\text{Hg}/\Delta^{201}\text{Hg} > 1$ has been determined on samples containing predominantly MeHg, for instance, biota samples, whereas $\Delta^{199}\text{Hg}/\Delta^{201}\text{Hg} \approx 1$ has been observed in environmental samples (e.g., sediments, water) containing predominantly Hg(II) (Tsui et al. 2020).

2.4. Stable isotopes of carbon and nitrogen analysis

Stable isotopic analyses for carbon and nitrogen were carried out at the Scientific and Technological Centers of the University of Barcelona (Spain). 0.30-0.35 mg of feather powder were placed into tin capsules and analyzed using a Thermo-Finnigan Flash 1112 elemental analyser (CE Elantech, Lakewood, NJ, USA) coupled to a Delta-C isotope ratio mass spectrometer via a CONFLO III interface (Thermo Finnigan MAT, Bremen, Germany). Stable isotope signatures are expressed using the standard delta notation relative to Vienna Pee Dee

Belemnite ($\delta^{13}C$) and atmospheric nitrogen ($\delta^{15}N$). IAEA standards (IAEA CH_7, IAEA CH_6, USGS 24 for ^{13}C, and IAEA N_1, IAEA N_2, IAEA NO_3 for ^{15}N) were applied every 12 samples to calibrate the system. Replicate assays of standards indicated analytical measurement errors of ± 0.1‰ and ± 0.2‰ for $\delta^{13}C$ and $\delta^{15}N$, respectively.

2.5. Statistical analyses

THg values and stable isotopes signatures ($\delta^{202}Hg$, $\Delta^{199}Hg$, $\Delta^{201}Hg$, $\Delta^{200}Hg$, $\Delta^{204}Hg$, $\delta^{13}C$, $\delta^{15}N$) were visually inspected to assess normality. THg values were log-transformed to approximate residual normality. Homogeneity of variances was tested using the Breusch-Pagan test.

2.5.1. Total mercury and stable isotopes signatures in Laridae *species*

ANOVA tests were performed to test differences among the three species studied (IA, CR and SH) in THg, $\delta^{202}Hg$, $\Delta^{199}Hg$, $\Delta^{201}Hg$, $\Delta^{200}Hg$ and $\Delta^{204}Hg$, $\delta^{13}C$ and $\delta^{15}N$ observed in feathers. Further pairwise comparisons were evaluated using Tukey tests. A linear model was fitted in order to evaluate the association between logTHg (response variable) and $\delta^{13}C$, $\delta^{15}N$ and Species and the interactions $\delta^{13}C$ × Species and $\delta^{15}N$ × Species as covariates.

Intraspecific correlation tests were performed for each species for each of the mercury isotopic tracers and THg in feathers, each of the mercury isotopic tracers and $\delta^{13}C$, each of the mercury isotopic tracers and $\delta^{15}N$. For the correlations analyses we omitted a data point from Audouin's gull that was an outlier in terms of $\delta^{13}C$ and affected the significance of the correlations test.

Linear models were fitted to estimate the slopes of $\Delta^{199}Hg/\delta^{202}Hg$, $\Delta^{199}Hg/\Delta^{201}Hg$ and $\Delta^{200}Hg/\Delta^{204}Hg$ for all the species studied.

2.5.2. Temporal changes in total mercury and stable isotope signatures in Audouin's gull fledglings

ANOVA tests were performed to test the differences in THg, δ^{202}Hg, Δ^{199}Hg, Δ^{201}Hg and δ^{15}N observed in feathers among years studied (2010, 2013, 2014, 2017). Further pairwise comparisons were evaluated using Tukey tests. Since assumptions of normality and homogeneity of variances were not met for δ^{13}C residuals, Kruskal Wallis test was used to examine the among years differences for δ^{13}C values and Wilcoxon Rank Sum Test for pairwise comparisons.

A linear mixed effects model was fitted to evaluate the association between log THg (response variable) and δ^{13}C, δ^{15}N (covariates), with year as a random effect. Correlation tests were used to assess correlations between each of the mercury isotopic tracers and THg in feathers, δ^{13}C, and δ^{15}N for each of the years studied and for all the years studied.

Besides, a linear model was fitted to test de association between Δ^{199}Hg and δ^{202}Hg. Finally, a linear model of Δ^{199}Hg as a response variable and Δ^{201}Hg as covariate was fitted to estimate the slope Δ^{199}Hg/Δ^{201}Hg for the years considered in the study (data for all the years pooled in a single dataset; for the regressions for each year see Supplementary Materials). In this linear model one extreme value was omitted from the dataset.

All statistical analyses used a significance level of α=0.05. Summary statistics are reported as mean ± SD, unless otherwise stated. All statistical analyses were performed using R v.4.0.3 (R Core Team 2020).

3. Results

3.1. Species differences in total mercury concentrations and isotopic composition

3.1.1. Total mercury concentrations

We analyzed feather samples from 10 individuals sampled in 2017 breeding season for each of the species of study (Audouin's gull (IA), black-headed gull (CR), common tern (SH)). Table 1 shows the mean ± SD for each of the variables studied. Significant differences in THg concentrations in fledglings' feathers were observed among species ($F_{2,27} = 167.64$, $p < 0.0001$; Fig. 1). Post-hoc tests showed significant differences among the three species considered (Fig.

1). Mean THg concentrations in feathers observed was greater for IA, followed by SH, and CR fledglings (Table 1).

3.1.2. Carbon and nitrogen stable isotopes and total mercury concentrations

Significant differences in both $\delta^{13}C$ and $\delta^{15}N$ were observed among species ($\delta^{13}C$: $F_{2,27} = 68.64$, $p < 0.0001$ and $\delta^{15}N$: $F_{2,27} = 29.02$, $p < 0.0001$). Post-hoc pairwise comparisons showed significant differences in $\delta^{13}C$ between IA-CR ($p < 0.0001$) and CR-SH ($p < 0.0001$), but not between IA-SH ($p = 0.29$) with $\delta^{13}C$ values being (IA ≈ SH) > CR (Fig. 2). Regarding $\delta^{15}N$ values, we detected differences between IA-SH ($p < 0.0001$) and CR-SH ($p < 0.0001$), but not between IA-CR ($p = 0.48$). $\delta^{15}N$ values were higher in IA and CR than SH (Fig. 2).

The linear model did not show a significant association between $\delta^{15}N$ or $\delta^{13}C$ and the observed THg levels in feathers ($\delta^{15}N$: $F_{1,21} = 0.025$, $p = 0.88$; $\delta^{13}C$: $F_{1,21} = 0.004$, $p = 0.95$). The interaction terms in the model had no effect on THg levels ($\delta^{15}N$ x Species: $F_{2,21} = 0.52$, $p = 0.60$; $\delta^{13}C$ x Species: $F_{2,21} = 1.22$, $p = 0.32$).

3.1.3. Mercury stable isotopes composition

Regarding mercury stable isotopes we found significant interspecific differences for $\delta^{202}Hg$ values ($F_{2,27} = 101.50$, $p < 0.0001$), $\Delta^{199}Hg$ ($F_{2,27} = 198.41$, $p < 0.0001$) and $\Delta^{201}Hg$ ($F_{2,27} = 181.49$, $p < 0.0001$). Post-hoc pairwise comparisons showed significant differences among the three species for $\delta^{202}Hg$ (all comparisons: $p < 0.0001$; Fig. 3) and between SH and CR, and CR and IA, but not between IA and CR for both $\Delta^{199}Hg$ (IA-SH: $p < 0.0001$; CR-SH: $p < 0.0001$; IA-CR: $p = 0.53$; Fig. 3) and $\Delta^{201}Hg$ (IA-SH: $p < 0.0001$; CR-SH: $p < 0.0001$; IA-CR: $p = 0.50$). Finally, no significant differences were found among species for $\Delta^{200}Hg$ ($F_{2,27} = 1.99$, $p = 0.15$) or $\Delta^{204}Hg$ ($F_{2,26} = 1.12$, $p = 0.34$).

Regression of $\Delta^{199}Hg$ against $\delta^{202}Hg$ showed a significant positive relationship ($F_{1,24} = 144.37$, $p < 0.0001$; Fig. 3), with a regression slope of 2.21. The ratio obtained from the regression between odd-MIF values $\Delta^{199}Hg/\Delta^{201}Hg$ for the three species studied was 1.16 (Fig.S1). The ratio between $\Delta^{200}Hg/\Delta^{204}Hg$ was not significantly different from 0 (Fig. S2).

Correlations among Hg stable isotopes and THg, $\delta^{15}N$ and $\delta^{13}C$, for each of the species are shown in Table 2.

3.2. Temporal variation in stable isotopic composition in Audouin's gull fledglings

3.2.1. Total mercury concentrations

Along the IA samples (N = 10 indivduals) analyzed in 2017, we also determined the THg in feathers from 10 IA fledglings in 2010, 2013, 2014, for a total of 40 feather samples (Table 3). We found significant differences among years ($F_{3,36} = 55.24$, $p < 0.0001$). Post-hoc pairwise comparisons detected significant differences among all year's pairs except 2014-2017 (Fig. 4). Mean THg concentrations in Audouin's gull fledgling feathers were higher in 2017≈2014>2010>2013 (Table 3).

3.2.2. Carbon and nitrogen stable isotopes and total mercury concentrations

Significant differences were observed for $\delta^{13}C$ values ($H = 10.16$, $p = 0.017$) and $\delta^{15}N$ values ($F_{3,36} = 32.90$, $p < 0.0001$) among years. Multiple pairwise comparisons for $\delta^{13}C$ values in feathers showed significant differences between 2013-2014 ($p = 0.011$) and 2013-2017 ($p = 0.019$), but not for the rest of pairwise comparisons (2010-2013: $p = 0.22$; 2010-2014: $p = 0.12$; 2010-2017: $p = 0.052$; 2014-2017: $p = 0.50$; Fig. 5). Pairwise comparisons for $\delta^{15}N$ signatures showed significant differences among all years' pairs ($p < 0.0001$ in all cases), except 2010-2013 ($p = 1.00$) and 2014-2017 ($p = 0.96$; Fig. 5), with $\delta^{15}N$ values higher in 2014 and 2017 than in 2010 and 2013 (Table 3).

The linear mixed effects model did show a significant association between $\delta^{13}C$ and the observed THg levels in feathers ($F_{1,34} = 5.20$, $p = 0.029$). Nonetheless, no significant association was observed between $\delta^{15}N$ values and THg levels in feathers ($F_{1,34} = 1.29$, $p = 0.26$).

3.2.3. Mercury stable isotopes composition

We found significant differences among years for $\delta^{202}Hg$ values ($F_{3,36} = 25.30$, $p < 0.0001$), $\Delta^{199}Hg$ ($F_{3,36} = 11.68$, $p < 0.0001$) and $\Delta^{201}Hg$ ($F_{3,36} = 8.25$, $p = 0.0002$) in gulls' feathers. Post-

hoc pairwise comparisons showed significant differences for δ^{202}Hg signatures among all years' pairs ($p < 0.0001$) except the pairs 2013-2017 ($p = 0.30$) and 2010-2014 ($p = 1.00$). Regarding Δ^{199}Hg pairwise comparisons showed significant differences between 2010-2013 ($p = 0.02$), 2010-2017 ($p < 0.0001$) and 2014-2017 ($p = 0.001$), although no significant differences were detected among the other years' pairs (in all cases, $p > 0.05$). For Δ^{201}Hg values pairwise comparisons showed significant differences between years 2010-2017 ($p = 0.0003$) and 2014-2017 ($p = 0.003$), but not among the other years' pairs (in all cases, $p > 0.05$).

Regarding Δ^{200}Hg and Δ^{204}Hg, we found significant differences among species for Δ^{200}Hg ($F_{3,36} = 3.45$, $p = 0.026$) but not for Δ^{204}Hg ($F_{3,36} = 0.86$, $p = 0.47$). Post-hoc comparisons showed significant differences in Δ^{200}Hg values for 2010-2013 ($p = 0.037$) but not among the other years' pairs (in all cases, $p > 0.05$).

Regression of Δ^{199}Hg against δ^{202}Hg values showed a significant positive relationship ($F_{1,38} = 23.05$, $p < 0.0001$; Fig. 6). The ratio between odd-MIF values Δ^{199}Hg/Δ^{201}Hg for all the years was 1.09 (Fig. S3). The ratio between Δ^{200}Hg/Δ^{204}Hg was not significantly different from 0 (Fig. S4).

Correlations among mercury stable isotopes and THg, δ^{15}N and δ^{13}C, for each of the years and all the years pooled are shown in Table 4.

4. Discussion

4.1. Species differences in total mercury concentrations and isotopic composition

4.1.1. Total mercury concentrations

Fledglings from the three species studied (IA, CR and SH) presented differences in THg levels in feathers. IA fledglings feathers had higher mercury concentration than those from SH or CR. This would be related to the different trophic resources exploited by each species, as mercury is mainly acquired through diet. Although the three species coexist in the same area and their breeding colonies are few km apart, they have distinct trophic ecologies: IA and SH depend mainly on marine resources, whereas CR forage mainly on rice-fields. Moreover, IA and SH exploit different marine resources. Essentially, SH are epipelagic foragers (Cotín et al. 2011),

399 while IA are opportunistic foragers on fisheries discards (Sanpera et al. 2007; García-Tarrasón
400 et al. 2015). Besides, IA also forage in terrestrial and freshwater environments (e.g., rice-fields;
401 Oro et al. 1996; Ruiz et al. 1996; Pedrocchi et al. 2002; Sanpera et al. 2007).
402
403 *4.1.2. Mercury, carbon and nitrogen stable isotopes*
404
405 Differences among the three species were found for δ^{202}Hg, whereas Δ^{199}Hg and Δ^{201}Hg only
406 differed between SH and IA, and between SH and CR. The differences observed for the odd-
407 MIF and MDF signatures might reflect differences in sources of mercury, the distinct trophic
408 ecologies among species, and differences among processes linked to Hg speciation among
409 foraging environments. Differences in Δ^{200}Hg and Δ^{204}Hg signatures were not observed among
410 the three species.
411
412 Δ^{199}Hg values reflect differences in MeHg sources owing to photodemethylation in the water
413 column (Bergquist and Blum 2007). Since odd-MIF signatures are maintained along the food
414 webs (Kwon et al. 2012), they reflect the foraging habitats from which fledglings of the
415 different species are fed. SH consumed epipelagic resources, where the incidence of sunlight
416 and photodemethylation processes predominate, leading to larger odd-MIF values (Blum et al.
417 2013; Bonsignore et al. 2015; Renedo et al. 2018). Conversely, IA are fed mainly on benthic
418 and mesopelagic species from fisheries discards (Sanpera et al. 2007; García-Tarrasón et al.
419 2013), for which the incidence of sunlight and thus photodemethylation rates are not as high
420 (Blum et al. 2013). As such, odd-MIF signatures observed in AI fledglings' feathers will be
421 lower. Analogously, CR feed juveniles with rice-field preys associated to the paddy soils (e.g.,
422 crayfish). In this case, possibly due to rice canopy and the turbidity of waters in rice paddies,
423 photochemical reactions are not enhanced in these environments (Gantner et al. 2009; Senn et
424 al. 2010; Sherman and Blum 2013), resulting in low odd-MIF values in CR fledglings' feathers.
425
426 The information obtained from the Hg stable isotopic signatures regarding the trophic ecology
427 for each species is consistent with the information obtained from the trophic markers. δ^{13}C
428 values are regarded as a proxy of carbon sources in diet and δ^{15}N is a proxy of trophic position
429 (Post et al. 2002). IA fledglings are feed mainly on benthic and mesopelagic discarded fish
430 which have higher trophic levels (e.g., Pedrocchi et al. 2002) resulting in higher δ^{15}N than SH,
431 which are fed mainly with epipelagic fish species of lower trophic levels (Cotín et al. 2011).
432 δ^{15}N values in CR fledglings are similar to those observed in IA. Nevertheless, it is important

to consider that the application of fertilizers in agricultural fields might be increasing $\delta^{15}N$ in these environments' food webs (Herbert and Wasseenar 2001; Cole et al. 2004). Therefore, CR nitrogen signatures need to be interpreted with caution, since they might not reflect accurately their trophic position, when comparing species across habitats. The $\delta^{13}C$ signatures observed in each of the three species are consistent with the foraging habitats for each of the species, with IA and SH fledglings presenting higher values than CR fledglings, associated to trophic sources from marine environments (García-Tarrasón et al. 2013). Conversely, the lower $\delta^{13}C$ signatures observed in CR fledglings, are similar to those found in other avian species in the area foraging freshwater habitats (Cotín et al. 2011).

Rice-fields are flooded with water coming from the Ebro river, that transports anthropogenic Hg downstream from the chlor-alkali site (Palanques et al. 2020). Generally, significant MIF has not been observed during river transport of Hg downstream (e.g., Washburn et al. 2017; Schudel et al. 2018; Reinfelder and Janssen 2019). Thus, we would expect CR fledglings will present odd-MIF signatures closer to those from the polluted site. And since IA fledglings present odd-MIF signatures similar to those from CR, this could point out that part of its mercury has a continental origin from the sediments transported by the river as influenced by the upstream polluted site. Indeed, although marine sedimentary Hg is often dominated by Hg of geogenic origin (e.g., volcanic activity, cinnabar deposits), surface layers of marine sediments have been shown to retain anthropogenic contributions (Ogrinc et al. 2019). Therefore, it is possible that anthropogenic mercury transported by the river has been deposited over decades in the sea sediment (Gustin et al. 2020), and it has accessed the benthic/mesopelagic food web (Perrot et al. 2010; Bonsignore et al. 2015), from which IA fledglings are fed. This observation is consistent with several studies, that have reported in sediments and biota from polluted sites, MIF signatures are close to 0‰ (eKwon et al. 2014; Wiederhold et al. 2015; Feng et al. 2019).

The species studied presented a $\Delta^{199}Hg/\Delta^{201}Hg$ slope of 1.17 (Fig. S1). $\Delta^{199}Hg/\Delta^{201}Hg$ ratios are used to identify mechanisms involving MIF variations. Also, they are assumed to be preserved along food webs biomagnification after MeHg assimilation by primary producers (Bergquist and Blum 2007). Experimentally theoretical $\Delta^{199}Hg/\Delta^{201}Hg$ slopes have been determined for aquatic systems, being for MeHg photodemethylation 1.36 (±0.02, 2 SE) and 1.00 (±0.02, 2 SE) for inorganic Hg photoreduction (Bergquist and Blum 2007). Several studies reported in marine and freshwater biota $\Delta^{199}Hg/\Delta^{201}Hg$ slopes higher than 1.00 and slightly

lower than 1.30 (e.g., Senn et al. 2010; Gehrke et al. 2011; Point et al. 2011; Day et al. 2012; Renedo et al. 2018). This deviation from the experimentally determined slopes is probably due to the organic ligands binding of Hg in the freshwater or marine environments (Bergquist and Blum 2007; Zheng and Hintelmann 2009).

In the case of MDF (δ^{202}Hg) values, both CR and IA were significantly lower (IA: 0.26±0.10; CR: 0.57±0.17) than those from SH (1.05±0.09) and are closer to 0‰. Although odd-MIF is much more sensible to photochemical reactions, the higher positive MDF values observed in SH feathers might reflect photochemical demethylation of MeHg in the photic zone of the marine water column, leaving a residual MeHg enriched in δ^{202}Hg (Blum et al. 2013; Bonsignore et al. 2015; Renedo et al. 2018) compared to CR and IA. Also, MDF signatures in fish from estuarine freshwater ecosystems compared to marine environments are shown to be more negative (Li et al. 2016). Thus, this reflects the trophic ecologies of CR and IA, and the influence of Hg derived from terrestrial/freshwater environments in the diet of IA fledglings. We also detected significant differences in MDF signatures between CR and IA, with IA δ^{202}Hg values being lower than CR values (Fig. 3). These differences possible arise from the impact of Hg legacy pollution from the chlor-alkali industry. Indeed, Cransveld et al. (2017) compared sea bass (*Dicentrarchus labrax*) populations among coastal polluted areas, and those subject to local chlor-alkali derived Hg pollution, presented higher δ^{202}Hg signatures than those in which background atmospherically Hg-contamination was assumed to constitute the main driver of δ^{202}Hg values. Chlor-alkali processes induce MDF, which help to trace Hg coming from industrial waste waters (Wiederhold et al. 2015). Although this possibly explains the higher MDF values of CR fledglings compared to those from IA fledglings we cannot rule out other factors that could be modifying MDF values and that would need further studying (e.g., trophic transfer (Laffont et al. 2009; Perrot et al. 2010, but see Kwon et al. 2012), metabolic reactions or physiological processes from the individual (Renedo et al. 2021).

The regression between Δ^{199}Hg and δ^{202}Hg values, showed a significant positive relationship with a slope of 2.21. This value is similar to those reported in previous studies, for lake and marine organisms (Berquist and Blum 2007; Motta et al. 2019; Kwon et al. 2020), and consistent with experimental studies, reporting increasing δ^{202}Hg and Δ^{199}Hg in remaining MeHg during photodegradation (Bergquist and Blum 2007), thus, implying a benthic-epipelagic gradient.

Finally, Δ^{200}Hg values are consistent with those reported in previous studies using seabirds as model organisms (Point et al. 2011; Day et al. 2012) and in Mediterranean biota (Jiskra et al. 2021). These signatures have been used to trace atmospheric inputs of Hg via precipitation. In precipitation samples, Δ^{200}Hg/Δ^{204}Hg ratio has been observed to be of -0.2 (Kwon et al. 2020). In our study, although it was negative, it was not significantly different from 0. Possibly, even-MIF values might be influenced by other sources of contamination, trophic transfers or other environmental factors that might be modifying the slope between these two isotopic tracers observed in precipitation samples (Kwon et al. 2020).

Correlation analyses did not show significant correlations for any of the species studied between MDF and THg, δ^{13}C or δ^{15}N in feathers. This reflects the fact that MDF mercury isotopic signatures are not only affected by the trophic ecology of the individuals and biomagnification processes along food webs (Laffont et al. 2009; Perrot et al. 2010) but also intrinsic metabolism and physiological processes, especially in high trophic level organisms (Laffont et al. 2009; Jackson 2018; Rua-Ibarz et al. 2019; Tsui et al. 2020; Renedo et al. 2020; 2021) and other environmental factors, including differences in Hg dynamics and fractionation on rice-paddies (e.g., Yin et al. 2013; Qin et al. 2020) *vs.* marine environments (e.g., Archer and Blum 2018), which need further study and are beyond the scope of the present work. However, Hg levels in feathers of SH did correlate negatively with odd-MIF values (Δ^{199}Hg and Δ^{201}Hg), but not for IA or CR fledglings. The negative correlation observed might appear since, even if major diet items foraged by common terns in the colony studied to feed their chicks are epipelagic fish species (Arcos et al. 2002), some of the individuals might also rely on mesopelagic/demersal resources obtained from fisheries discards (Guitart et al. 2003; Cotín et al. 2011). This is consistent with a higher variability in odd-MIF signatures in this species. Conversely, both gulls' species present low odd-MIF variability (Fig. 3). Finally, we found positive correlations between δ^{13}C and odd-MIF values in CR and IA (Table 2). These positive correlations are in accordance to those reported in guillemots (*Uria aalge* and *U. lomvia*) breeding in the Alaskan Artic, which was attributed to a δ^{13}C gradient from terrestrial to oceanic systems' sources and a lower photochemical demethylation in coastal systems due to higher turbidity (Day et al. 2012). In our study, these positive correlations might reflect individual variability within species in dietary sources with different proportions of continental and coastal marine resources, especially in IA (Sanpera et al. 2007; García-Tarrasón et al. 2015).

Thus, mercury stable isotopes confirm the trophic ecologies for the species under study and point out a possible influence of Hg from anthropogenic origin in IA fledglings, as signatures are similar to those in CR fledglings. Furthermore, they distinguish the foraging ecologies in a vertical gradient of IA and SH, with IA consuming mainly benthic/mesopelagic species and SH consuming epipelagic fish.

4.2. Temporal variation in stable isotopic signatures in Audouin's gull fledglings

4.2.1. Total mercury concentrations

Total mercury concentrations in the Audouin's gull colony varied among years (Fig. 4). Previous studies in this colony (Sánchez-Fortún et al. 2020), have suggested this could be related to the sediment dragging that took place in 2013-2014 in the site next to the chlor-alkali plant, which remobilized legacy mercury. In the present study, Hg levels were 2017≈2014>2010>2013. This is consistent with the results obtained by Sánchez-Fortún et al. (2020) for a longer time series from the same breeding colony using larger sample sizes. Accordingly, we would expect that the mercury found in 2014 is predominantly mercury sourced from the chlor-alkali plant surroundings that has been transported through the river. The peak in THg in feathers of Audouin's gull fledglings in 2017 could be attributed to the deposition over time of mercury transported by the river on the coastal seabed (Palanques et al. 2020).

4.2.2. Mercury, carbon and nitrogen stable isotopes

We found differences in both $\delta^{13}C$ and $\delta^{15}N$ stable isotopes signatures in feathers among years. The $\delta^{13}C$ signatures from 2010, 2014 and 2017 are consistent with carbon stable isotopes signatures from marine environments (Fig. 5; García-Tarrasón et al. 2013; Sánchez-Fortún et al. 2020). Individuals from 2013 presented the largest range of $\delta^{13}C$ values, indicating significant differences in carbon sources among the individuals sampled. According to the $\delta^{13}C$ observed in 2013 at least 3 individuals were being fed predominantly with rice-field sources (Fig. 5), with their $\delta^{13}C$ ranging from -19.7 to -24.1‰. This is consistent with this and other studies in the area using aquatic birds feeding from freshwater resources (e.g., black-headed gull [Table 1, this study], Cotín et al. 2011). $\delta^{13}C$ values were positively associated with THg

values in feathers, accounting for the different dietary proportions from rice-fields or marine environments, with individuals fed with higher proportions of rice-field preys (lower $\delta^{13}C$), having lower THg levels in feathers (García-Tarrasón et al. 2013).

Regarding $\delta^{15}N$ signatures, there were clear differences between 2010 vs. 2013, and 2014 vs. 2017, although we did not detect any association with THg levels in feathers. In this colony, it has been observed, that besides a possible pollution episode derived from the cleansing of the chlor-alkali plant site in 2013-2014, a parallel eutrophication process could have been occurred, as suggested by Sánchez-Fortún et al. (2020) in a longitudinal study using compound specific stable isotopes of nitrogen, which might variate baseline $\delta^{15}N$ over time influencing the consumer's $\delta^{15}N$ (Cole et al. 2004), thus not reflecting the actual trophic position of the individuals if comparing the values among years.

Mercury stable isotopes showed differences among years for $\delta^{202}Hg$, $\Delta^{199}Hg$ and $\Delta^{201}Hg$ values. Regarding $\Delta^{199}Hg$, the year 2017 presented the lowest values among the years studied, followed by 2013, 2014 which presented similar values, and 2010 with the highest values, although statistically significant differences were not always detected due to intra-annual variability in individual signatures. $\Delta^{199}Hg$ in 2017 ranged from 0.60–1.11‰, whereas in 2010 from 1.12–1.45‰, in 2013 from 0.85–1.25‰ and in 2014 from 0.92–1.49‰. $\Delta^{199}Hg$ (and $\Delta^{201}Hg$) showed a significant negative correlation with THg when pooling the data for all the years (Table 4). Since individuals being fed with more proportion of fisheries discards (mesopelagic and benthic species) rather than epipelagic or freshwater/terrestrial sources will likely present higher levels of Hg in their bodies (García-Tarrasón et al. 2013) and lower odd-MIF isotopic composition (Blum et al. 2013) this might explain the negative correlation encountered. The $\Delta^{199}Hg/\Delta^{201}Hg$ slope obtained from the regression on this dataset was 1.09, which lays in between the experimentally derived slopes for Hg(II) photoreduction (~1.00) and MeHg photodemethylation (~1.30). The odd-MIF slope found for all the years in this study is consistent with the one found in common murre's eggs by Day et al. (2012), that was 1.09. However, with the existing knowledge on Hg fractionation in the environment, 1.09 is inconclusive in terms of the process leading to $\Delta^{199}Hg$ and $\Delta^{201}Hg$ signatures prior to the incorporation in the food web (Day et al. 2012). $\Delta^{199}Hg/\Delta^{201}Hg$ slopes signatures depend on a variety of factors such as DOC levels relative to Hg concentrations in the environment, type of DOC present and irradiance (Bergquist and Blum 2007; Zheng and Hintelmann 2009). In

natural conditions, these factors might develop an important role in determining $\Delta^{199}Hg/\Delta^{201}Hg$ slope, and for our samples, we assume they will vary widely among years and due to the complexity of the ecosystems under study.

No significant correlation was found between odd-MIF signatures and $\delta^{13}C$, possibly due to the low ranges observed in $\delta^{13}C$ values in the years studied, except for N = 3 individuals in 2013 which presented lower $\delta^{13}C$ values (Fig. 5). We found significant negative correlation between MIF signatures and $\delta^{15}N$ values when considering the data for all the years (Table 4). However, due to $\delta^{15}N$ variations in food webs baselines over years, interpretations on this correlation in terms of trophic levels might be misleading (Sánchez-Fortún et al. 2020). Nonetheless, even if data on Hg stable isotopes from the polluted site at Flix is not available, for all the years studied, odd-MIF values range from 0.60–1.49‰. These values seem to indicate that overall, there might be an influence of Hg proceeding from the polluted site in the Audouin's gull colony in the Ebro Delta over the years in a varying degree.

Regarding even-MIF values, for the years considered in this study, the $\Delta^{200}Hg/\Delta^{204}Hg$ ratio in IA fledglings feathers was not significantly different from 0. This might be indicative of other sources of contamination, trophic transfers or other environmental factors that might be modifying the slope between these two isotopic tracers found in global precipitation samples (-0.2; Kwon et al. 2020).

Interestingly, MDF ($\delta^{202}Hg$) in Audouin's gull fledgling feathers presented similar values between 2013 and 2017 (mean ± SD: 0.20±0.11) and between 2010 and 2014 (mean ± SD: 0.60±0.18), being MDF values in 2010 and 2014 higher than those from 2013 and 2017. Since $\delta^{202}Hg$ values were not correlated with $\delta^{15}N$ nor $\delta^{13}C$, this $\delta^{202}Hg$ difference among years was not due to an altered trophic ecology (i.e., as a result of trophic level exploited [Point et al. 2011; Tsui et al. 2020]). Furthermore, MDF values for 2010 and 2014 are closer to those obtained for CR in this study (mean ± SD: 0.57±0.17), a species more impacted by anthropogenic derived mercury.

Several studies in the Ebro river and the Ebro Delta area pointed out the possible influence of the presence of the Flix chlor-alkali plant on Hg levels in biota (Sanpera et al. 2007; Faria et al. 2010; Cotín et al. 2011; Carrasco et al. 2011; Sánchez-Fortún et al. 2020). The phase-down of activities using Hg in the plant started in 2004 with a consequent decrease in Hg emissions

(Pujadas 2016), until the complete cessation of them in 2017. In 2013 a management plan to remediate the contaminated soils nearby the chlor-alkali site was performed, which could have had an impact on biota downstream the river, due to mobilization of legacy mercury. From 2004 to 2013, in the Audouin's gull colony in the Ebro Delta a progressive decrease in Hg levels in feathers of fledglings has been described, followed by a slightly increase from 2014 onwards (Sánchez-Fortún et al. 2020). Thus, we expected the Audouin's gull colony in the years 2010 and 2014 to be affected by a major extent with Hg transported from the chlor-alkali plant site, while in 2013 and 2017 would be less impacted by anthropogenic pollution due to ecosystem recovery (Kopec et al. 2019). The results of the present study regarding MDF values on these years seem to be consistent with this idea, with individuals presenting higher MDF values in 2010 and 2014, associated to higher influence of chlor-alkali derived Hg (Cransveld et al. 2017; Feng et al. 2019).

Nonetheless, although we did find a weak positive correlation between δ^{202}Hg and THg levels in feathers, which would reinforce the idea of an increase of δ^{202}Hg coupled to the additional pollution from the chlor-alkali site, it was not significant ($r = 0.29$; $p = 0.07$). Unfortunately, with the available data we are not able to discern among the possible factors and sources leading to the different concentrations in total mercury in feathers from the different years. Possibly, river dynamics over decades has had an influence in transporting Hg from the polluted site towards the coastal seabed sediments surrounding the colony (Palanques et al. 2020), which would lead to an increase in Hg on the marine food web (e.g., Sánchez-Fortún et al. 2020), although other factors not taken into account in this study (e.g., physiology of species; Renedo et al. 2020, 2021; fractions of inorganic mercury and MeHg accumulated in organisms; Pinzone et al. 2021) and the complexity of estuarine environments could be influencing THg levels or MDF signatures, and thus, modifying the correlation between MDF and THg values.

5. Conclusions

Stable isotopes of mercury have been shown to be a promising tool in investigating processes and sources leading to Hg body burdens in biota. In this study we applied this methodology to understand differences in Hg levels observed in three species of seabirds breeding in the Ebro Delta area (NE Iberian Peninsula), which has been long impacted by the legacy mercury pollution from a chlor-alkali plant. Furthermore, we have also investigated how temporal

changes in anthropogenic activities leading to Hg release or remobilization in the environment can be traced by Hg stable isotopes measured in a bioindicator species such as the Audouin's gull. Nonetheless, due to complexity of ecosystems, trophic ecology, physiology of species and other processes affecting mercury isotopic signatures, particularly MDF, more studies in this direction should be performed in order to be able to discern processes related to Hg accumulation in top-predators foraging in complex ecosystems such as wetlands and marine environments.

Acknowledgements

We would like to thank all the personnel at the Ebro Delta Natural Park, field and lab technicians for their work on sample collection and preparation, and the personnel at the Scientific and Technical Centers of the Universitat de Barcelona for their help in stable isotopes of C and N preparation and analysis, and the lab technicians at IPREM for their assistance during Hg isotopic analyses. The present work was funded by project CGL2016-80963R (Ministerio de Economía y Competividad, Spain).

References

ACA (Agència Catalana de l'Aigua). (2013). *Descontaminació a l'embassament de Flix. Resum Executiu.* https://aca-web.gencat.cat/aca/documents/ca/Gestio_medi/Resum_executiu.pdf

Albert, C., Renedo, M., Bustamante, P., & Fort, J. (2019). Using blood and feathers to investigate large-scale Hg contamination in Arctic seabirds: A review. *Environmental Research*, *177*. https://doi.org/10.1016/j.envres.2019.108588

Amos, H. M., Jacob, D. J., Streets, D. G., & Sunderland, E. M. (2013). Legacy impacts of all-time anthropogenic emissions on the global mercury cycle. *Global Biogeochemical Cycles*, *27*, 410–421. https://doi.org/10.1002/gbc.20040

Antón-Tello, M., Britto, V. O., Gil-Delgado, J. A., Rico, E., Dies, J. I., Monrós, J. S., & Vera, P. (2021). Unravelling diet composition and niche segregation of colonial waterbirds in a Mediterranean wetland using stable isotopes. *Ibis*, ibi.12928. https://doi.org/10.1111/ibi.12928

Archer, D. E., & Blum, J. D. (2018). A model of mercury cycling and isotopic fractionation in the ocean. *Biogeosciences*, *15*, 6297–6313. https://doi.org/10.5194/bg-15-6297-2018

Arcos, J. M., Ruiz, X., Bearhop, S., & Furness, R. W. (2002). Mercury levels in seabirds and their fish prey at the Ebro Delta (NW Mediterranean): the role of trawler discards as a source of contamination. *Marine Ecology Progress Series*, *232*, 281–290. https://doi.org/10.3354/meps232281

Bearhop, S., Waldron, S., Thompson, D., & Furness, R. (2000). Bioamplification of mercury in great skua *Catharacta skua* chicks: The influence of trophic status as determined by stable isotope signatures of blood and feathers. *Marine Pollution Bulletin*, *40*(2), 181–185. https://doi.org/10.1016/S0025-326X(99)00205-2

Becker, P. H., González-Solís, J., Behrends, B., & Croxall, J. (2002). Feather mercury levels in seabirds at South Georgia: Influence of trophic position, sex and age. *Marine Ecology Progress Series*, *243*, 261–269. https://doi.org/10.3354/meps243261

Bergquist, B. A., & Blum, J. D. (2007). Mass-dependent and -independent fractionation of Hg isotopes by photoreduction in aquatic systems. *Science*, *318*, 417–420. https://doi.org/10.1126/science.1148050

Blévin, P., Carravieri, A., Jaeger, A., Chastel, O., Bustamante, P., & Cherel, Y. (2013). Wide Range of Mercury Contamination in Chicks of Southern Ocean Seabirds. *PLoS ONE*, *8*. https://doi.org/10.1371/journal.pone.0054508

Blum, J. D., Popp, B. N., Drazen, J. C., Choy, C. A., & Johnson, M. W. (2013). Methylmercury production below the mixed layer in the North Pacific Ocean. *Nature Geoscience*, *6*, 879–884. https://doi.org/10.1038/ngeo1918

721 Boecklen, W. J., Yarnes, C. T., Cook, B. A., & James, A. C. (2011). On the use of stable
722 isotopes in trophic ecology. *Annual Review of Ecology, Evolution, and Systematics*, *42*,
723 411–440. https://doi.org/10.1146/annurev-ecolsys-102209-144726

724 Bond, A. L., & Diamond, A. W. (2009). Total and methyl mercury concentrations in seabird
725 feathers and eggs. *Archives of Environmental Contamination and Toxicology*, *56*(2),
726 286–291. https://doi.org/10.1007/s00244-008-9185-7

727 Bond, A. L., & Lavers, J. L. (2020). Biological archives reveal contrasting patterns in trace
728 element concentrations in pelagic seabird feathers over more than a century.
729 *Environmental Pollution*, *263*, 114631. https://doi.org/10.1016/j.envpol.2020.114631

730 Bonsignore, M., Tamburrino, S., Oliveri, E., Marchetti, A., Durante, C., Berni, A., Quinci, E.,
731 & Sprovieri, M. (2015). Tracing mercury pathways in Augusta Bay (southern Italy) by
732 total concentration and isotope determination. *Environmental Pollution*, *205*, 178–185.
733 https://doi.org/10.1016/j.envpol.2015.05.033

734 Bowman, K. L., Lamborg, C. H., & Agather, A. M. (2020). A global perspective on mercury
735 cycling in the ocean. *Science of the Total Environment*, *710*.
736 https://doi.org/10.1016/j.scitotenv.2019.136166

737 Burger, J., & Gochfeld, M. (2004). Marine Birds as Sentinels of Environmental Pollution.
738 *EcoHealth*, *1*, 263–274. https://doi.org/10.1007/s10393-004-0096-4

739 Campillo, J. A., Santos-Echeandía, J., & Fernández, B. (2019). The hydrological regime of a
740 large Mediterranean river influences the availability of pollutants to mussels at the
741 adjacent marine coastal area: Implications for temporal and spatial trends. *Chemosphere*,
742 *237*. https://doi.org/10.1016/j.chemosphere.2019.124492

743 Carrasco, L., Barata, C., García-Berthou, E., Tobias, A., Bayona, J. M., & Díez, S. (2011).
744 Patterns of mercury and methylmercury bioaccumulation in fish species downstream of
745 a long-term mercury-contaminated site in the lower Ebro River (NE Spain).
746 *Chemosphere*, *84*(11), 1642–1649. https://doi.org/10.1016/j.chemosphere.2011.05.022

747 Carrasco, L., Bayona, J. M., & Díez, S. (2010). Mercury in Aquatic Organisms of the Ebro
748 River Basin. In D. Barceló & M. Petrovic (Eds.), *The Ebro River Basin, Hdb Env Chem.*
749 (Vol. 5, pp. 1–12). Springer-Verlag. https://doi.org/DOI 10.1007/698_2010_71

750 Celo, V., Lean, D. R. S., & Scott, S. L. (2006). Abiotic methylation of mercury in the aquatic
751 environment. *Science of the Total Environment*, *368*, 126–137.
752 https://doi.org/10.1016/j.scitotenv.2005.09.043

753 Clarkson, T. W., & Magos, L. (2006). The toxicology of mercury and its chemical
754 compounds. *Critical Reviews in Toxicology*, *36*(8), 609–662.
755 https://doi.org/10.1080/10408440600845619

756 Cole, M. L., Valiela, I., Kroeger, K. D., Tomasky, G. L., Cebrian, J., Wigand, C., Mckinney,
757 R. A., Grady, S. P., & Carvalho da Silva, M. H. (2004). Assessment of a $\delta^{15}N$ isotopic
758 method to indicate anthropogenic eutrophication in aquatic ecosystems. *J. Environ.*
759 *Qual.*, *33*, 124–132.

760 Cossa, D., & Coquery, M. (2005). The mediterranean mercury anomaly, a geochemical or a
761 biological issue. In A. Saliot (Ed.), The Mediterranean Sea. The Handbook of
762 Environmental Chemistry. (Vol. 5, Part K). Springer-Verlag, Berlin, Heidelberg.
763 https://doi.org/10.1007/b107147

764 Cotín, J., García-Tarrasón, M., Jover, L. & Sanpera, C. (2012). Are the toxic sediments
765 deposited at Flix reservoir affecting the Ebro river biota? Purple heron eggs and
766 nestlings as indicators. *Ecotoxicology*, *21*, 1391–1402. https://doi.org/10.1007/s10646-
767 012-0893-4

768 Cotín, J., García-Tarrasón, M., Sanpera, C., Jover, L., & Ruiz, X. (2011). Sea, freshwater or
769 saltpans? Foraging ecology of terns to assess mercury inputs in a wetland landscape:
770 The Ebro Delta. *Estuarine, Coastal and Shelf Science*, *92*, 188–194.
771 https://doi.org/10.1016/j.ecss.2010.12.024

772 Cransveld, A., Amouroux, D., Tessier, E., Koutrakis, E., Ozturk, A. A., Bettoso, N., Mieiro,
773 C. L., Bérail, S., Barre, J. P. G., Sturaro, N., Schnitzler, J., & Das, K. (2017). Mercury
774 Stable Isotopes Discriminate Different Populations of European Seabass and Trace
775 Potential Hg Sources around Europe. *Environmental Science and Technology*, *51*,
776 12219–12228. https://doi.org/10.1021/acs.est.7b01307

777 Day, R. D., Roseneau, D. G., Berail, S., Hobson, K. A., Donard, O. F. X., Vander Pol, S. S.,
778 Pugh, R. S., Moors, A. J., Long, S. E., & Becker, P. R. (2012). Mercury stable isotopes
779 in seabird eggs reflect a gradient from terrestrial geogenic to oceanic mercury reservoirs.
780 *Environmental Science and Technology*, *46*, 5327–5335.
781 https://doi.org/10.1021/es2047156

782 Driscoll, C. T., Mason, R. P., Chan, H. M., Jacob, D. J., & Pirrone, N. (2013). Mercury as a
783 global pollutant: Sources, pathways, and effects. *Environmental Science and*
784 *Technology*, *47*(10), 4967–4983. https://doi.org/10.1021/es305071v

785 Estrade, N., Carignan, J., & Donard, O. F. X. (2010). Isotope tracing of atmospheric mercury
786 sources in an urban area of Northeastern France. *Environmental Science and*
787 *Technology*, *44*, 6062–6067. https://doi.org/10.1021/es100674a

788 Evers, D. (2018). The Effects of Methylmercury on Wildlife: A Comprehensive Review and
789 Approach for Interpretation. In D. A. DellaSala & M. I. Goldstein (Eds.), *Encyclopedia*
790 *of the Anthropocene* (Vol. 5, pp. 181–194). Elsevier. https://doi.org/10.1016/b978-0-12-
791 809665-9.09985-7

792 Faria, M., Huertas, D., Soto, D. X., Grimalt, J. O., Catalan, J., Riva, M. C., & Barata, C.
793 (2010). Contaminant accumulation and multi-biomarker responses in field collected
794 zebra mussels (*Dreissena polymorpha*) and crayfish (*Procambarus clarkii*), to evaluate
795 toxicological effects of industrial hazardous dumps in the Ebro river (NE Spain).
796 *Chemosphere*, *78*, 232–240. https://doi.org/10.1016/j.chemosphere.2009.11.003

797 Feng, C., Pedrero, Z., Gentès, S., Barre, J., Renedo, M., Tessier, E., Berail, S., Maury-
798 Brachet, R., Mesmer-Dudons, N., Baudrimont, M., Legeay, A., Maurice, L., Gonzalez,
799 P., & Amouroux, D. (2015). Specific Pathways of Dietary Methylmercury and Inorganic
800 Mercury Determined by Mercury Speciation and Isotopic Composition in Zebrafish

(*Danio rerio*). *Environmental Science and Technology*, *49*, 12984–12993. https://doi.org/10.1021/acs.est.5b03587

Feng, C., Pedrero, Z., Lima, L., Olivares, S., de la Rosa, D., Berail, S., Tessier, E., Pannier, F., & Amouroux, D. (2019). Assessment of Hg contamination by a Chlor-Alkali Plant in riverine and coastal sites combining Hg speciation and isotopic signature (Sagua la Grande River, Cuba). *Journal of Hazardous Materials*, *371*, 558–565. https://doi.org/10.1016/j.jhazmat.2019.02.092

Furness, R. W., & Camphuysen, C. J. (1997). Seabirds as monitors of the marine environment. *ICES Journal of Marine Science*, *54*, 726–737. https://doi.org/10.1006/jmsc.1997.0243

Gantner, N., Hintelmann, H., Zheng, W., & Muir, D. C. (2009). Variations in stable isotope fractionation of Hg in food webs of Arctic lakes. *Environmental Science and Technology*, *43*, 9148–9154. https://doi.org/10.1021/es901771r

García-Tarrasón, M., Bécares, J., Bateman, S., Arcos, J. M., Jover, L., & Sanpera, C. (2015). Sex-specific foraging behavior in response to fishing activities in a threatened seabird. *Ecology and Evolution*, *5*, 2348–2358. https://doi.org/10.1002/ece3.1492

García-Tarrasón, M., Pacho, S., Jover, L., & Sanpera, C. (2013). Anthropogenic input of heavy metals in two Audouin's gull breeding colonies. *Marine Pollution Bulletin*, *74*(1), 285–290. https://doi.org/10.1016/j.marpolbul.2013.06.043

Gehrke, G. E., Blum, J. D., Slotton, D. G., & Greenfield, B. K. (2011). Mercury isotopes link mercury in San Francisco bay forage fish to surface sediments. *Environmental Science and Technology*, *45*, 1264–1270. https://doi.org/10.1021/es103053y

Grimalt, J. O., Sánchez-Cabeza, J. A., Palanques, A., & Catalan, J. (2003). *Estudi de la dinàmica dels compostos organoclorats persistents i altres contaminants en els sistemes aquàtics continentals*. Barcelona, Spain.

Guitart, R., Mateo, R., Sanpera, C., Hernández-Matías, A., & Ruiz, X. (2003). Mercury and selenium levels in eggs of common terns (*Sterna hirundo*) from two breeding colonies in the Ebro Delta, Spain. *Bulletin of Environmental Contamination and Toxicology*, *70*, 71–77. https://doi.org/10.1007/s00128-002-0157-8

Gustin, M. S., Bank, M. S., Bishop, K., Bowman, K., Branfireun, B., Chételat, J., Eckley, C. S., Hammerschmidt, C. R., Lamborg, C., Lyman, S., Martínez-Cortizas, A., Sommar, J., Tsui, M. T. K., & Zhang, T. (2020). Mercury biogeochemical cycling: A synthesis of recent scientific advances. *Science of the Total Environment*, *737*. https://doi.org/10.1016/j.scitotenv.2020.139619

Hebert, C. E., & Wassenaar, L. I. (2001). Stable nitrogen isotopes in waterfowl feathers reflect agricultural land use in western Canada. Environ. Sci. Technol., 35, 3482–3487. https://doi.org/10.1021/es001970p

Jackson, T. A. (2018). Isotopic and chemical characteristics of mercury in organs and tissues of fish in a mercury-polluted lake: Evidence for fractionation of mercury isotopes by

physiological processes. *Environmental Toxicology and Chemistry*, *37*, 515–529. https://doi.org/10.1002/etc.3987

Janssen, S. E., Schaefer, J. K., Barkay, T., & Reinfelder, J. R. (2016). Fractionation of Mercury Stable Isotopes during Microbial Methylmercury Production by Iron- and Sulfate-Reducing Bacteria. *Environmental Science and Technology*, *50*, 8077–8083. https://doi.org/10.1021/acs.est.6b00854

Jiskra, M., Heimbürger-Boavida, L. E., Desgranges, M. M., Petrova, M. V., Dufour, A., Ferreira-Araujo, B., Masbou, J., Chmeleff, J., Thyssen, M., Point, D., & Sonke, J. E. (2021). Mercury stable isotopes constrain atmospheric sources to the ocean. *Nature*, *597*, 678–682. https://doi.org/10.1038/s41586-021-03859-8

Kopec, A. D., Kidd, K. A., Fisher, N. S., Bowen, M., Francis, C., Payne, K., & Bodaly, R. A. (2019). Spatial and temporal trends of mercury in the aquatic food web of the lower Penobscot River, Maine, USA, affected by a chlor-alkali plant. *Science of the Total Environment*, *649*, 770–791. https://doi.org/10.1016/j.scitotenv.2018.08.203

Kritee, K., Barkay, T., & Blum, J. D. (2009). Mass dependent stable isotope fractionation of mercury during *mer* mediated microbial degradation of monomethylmercury. *Geochimica et Cosmochimica Acta*, *73*, 1285–1296. https://doi.org/10.1016/j.gca.2008.11.038

Kwon, S. Y., Blum, J. D., Carvan, M. J., Basu, N., Head, J. A., Madenjian, C. P., & David, S. R. (2012). Absence of fractionation of mercury isotopes during trophic transfer of methylmercury to freshwater fish in captivity. *Environmental Science and Technology*, *46*, 7527–7534. https://doi.org/10.1021/es300794q

Kwon, S. Y., Blum, J. D., Chen, C. Y., Meattey, D. E., & Mason, R. P. (2014). Mercury isotope study of sources and exposure pathways of methylmercury in estuarine food webs in the northeastern U.S. *Environmental Science and Technology*, *48*, 10089–10097. https://doi.org/10.1021/es5020554

Kwon, S. Y., Blum, J. D., Yin, R., Tsui, M. T.-K., Yang, Y. H., & Choi, J. W. (2020). Mercury stable isotopes for monitoring the effectiveness of the Minamata Convention on Mercury. *Earth-Science Reviews*, *203*. https://doi.org/10.1016/j.earscirev.2020.103111

Laffont, L., Sonke, J. E., Maurice, L., Hintelmann, H., Pouilly, M., Sánchez Bacarreza, Y., Perez, T., & Behra, P. (2009). Anomalous Mercury Isotopic Compositions of Fish and Human Hair in the Bolivian Amazon. *Environmental Science and Technology*, *43*, 8985–8990. https://doi.org/10.1021/es9019518

Laffont, L., Sonke, J. E., Maurice, L., Monrroy, S. L., Chincheros, J., Amouroux, D., & Behra, P. (2011). Hg speciation and stable isotope signatures in human hair as a tracer for dietary and occupational exposure to mercury. *Environmental Science and Technology*, *45*, 9910–9916. https://doi.org/10.1021/es202353m

Lavoie, R. A., Jardine, T. D., Chumchal, M. M., Kidd, K. A., & Campbell, L. M. (2013). Biomagnification of mercury in aquatic food webs: A worldwide meta-analysis.

Environmental Science and Technology, *47*(23), 13385–13394. https://doi.org/10.1021/es403103t

Li, M., Schartup, A. T., Valberg, A. P., Ewald, J. D., Krabbenhoft, D. P., Yin, R., Balcom, P. H., & Sunderland, E. M. (2016). Environmental Origins of Methylmercury Accumulated in Subarctic Estuarine Fish Indicated by Mercury Stable Isotopes. *Environmental Science and Technology*, *50*, 11559–11568. https://doi.org/10.1021/acs.est.6b03206

Lyman, S. N., Cheng, I., Gratz, L. E., Weiss-Penzias, P., & Zhang, L. (2020). An updated review of atmospheric mercury. *Science of the Total Environment*, *707*. https://doi.org/10.1016/j.scitotenv.2019.135575

Mañosa, S., Mateo, R., & Guitart, R. (2001). A review of the effects of agricultural and industrial contamination on the Ebro Delta biota and wildlife. *Environmental Monitoring and Assessment*, *71*, 187–205.

Morel, F. M. M., Kraepiel, A. M. L., & Amyot, M. (1998). The chemical cycle and bioaccumulation of mercury. *Annual Review of Ecology and Systematics*, *29*, 543–566. https://doi.org/10.1146/annurev.ecolsys.29.1.543

Ogrinc, N., Hintelmann, H., Kotnik, J., Horvat, M., & Pirrone, N. (2019). Sources of mercury in deep-sea sediments of the Mediterranean Sea as revealed by mercury stable isotopes. *Scientific Reports*, *9*, 1–9. https://doi.org/10.1038/s41598-019-48061-z

Oro, D., Genovart, X., Ruiz, X., Jimenez, J., & Garcia-Gans, J. (1996). Differences in Diet, Population Size and Reproductive Performance between Two Colonies of Audouin's Gull *Larus audouinii* Affected by a Trawling Moratorium. *Journal of Avian Biology*, *27*(3), 245–251. https://doi.org/10.2307/3677229

Palanques, A., Guillén, J., Puig, P., & Grimalt, J. O. (2020). Effects of flushing flows on the transport of mercury-polluted particulate matter from the Flix Reservoir to the Ebro Estuary. *Journal of Environmental Management*, *260*(December 2019). https://doi.org/10.1016/j.jenvman.2019.110028

Pedrocchi, V., Oro, D., González-Solís, J., Ruiz, X., & Jover, L. (2002). Differences in diet between the two largest breeding colonies of Audouin's gulls: The effects of fishery activities. *Scientia Marina*, *66*(3), 313–320. https://doi.org/10.3989/scimar.2002.66n3313

Perrot, V., Epov, V. N., Pastukhov, M. V., Grebenshchikova, V. I., Zouiten, C., Sonke, J. E., Husted, S., Donard, O. F. X., & Amouroux, D. (2010). Tracing sources and bioaccumulation of mercury in fish of Lake Baikal - Angara River using Hg isotopic composition. *Environmental Science and Technology*, *44*, 8030–8037. https://doi.org/10.1021/es101898e

Pinzone, M., Cransveld, A., Tessier, E., Bérail, S., Schnitzler, J., Das, K., & Amouroux, D. (2021). Contamination levels and habitat use influence Hg accumulation and stable isotope ratios in the European seabass Dicentrarchus labrax. *Environmental Pollution*, *281*. https://doi.org/10.1016/j.envpol.2021.117008

Podar, M., Gilmour, C. C., Brandt, C. C., Soren, A., Brown, S. D., Crable, B. R., Palumbo, A. V., Somenahally, A. C., & Elias, D. A. (2015). Global prevalence and distribution of genes and microorganisms involved in mercury methylation. *Science Advances*, *1*(9). https://doi.org/10.1126/sciadv.1500675

Point, D., Sonke, J. E., Day, R. D., Roseneau, D. G., Hobson, K. A., Vander Pol, S. S., Moors, A. J., Pugh, R. S., Donard, O. F. X., & Becker, P. R. (2011). Methylmercury photodegradation influenced by sea-ice cover in Arctic marine ecosystems. *Nature Geoscience*, *4*, 188–194. https://doi.org/10.1038/ngeo1049

Post, D. M. (2002). Using Stable Isotopes to Estimate Trophic Position: Models , Methods , and Assumptions. *Ecology*, *83*(3), 703–718.

Pujadas, M. (2016). Historia ambiental de la planta electroquímica de Flix: el Principio de Precaución frente al paradigma del crecimiento. *Revista de Historia Industrial*, *25*(62), 75–107.

Qin, C., Du, B., Yin, R., Meng, B., Fu, X., Li, P., Zhang, L., & Feng, X. (2020). Isotopic Fractionation and Source Appointment of Methylmercury and Inorganic Mercury in a Paddy Ecosystem. *Environmental Science and Technology*, *54*, 14334–14342. https://doi.org/10.1021/acs.est.0c03341

R Core Team. (2020). R: A language and environment for statistical computing. Vienna, Austria: R Foundation for Statistical Computing. Retrieved from https://www.r-project.org/

Regnell, O., & Watras, C. J. (2019). Microbial Mercury Methylation in Aquatic Environments: A Critical Review of Published Field and Laboratory Studies. *Environmental Science and Technology*, *53*, 4–19. https://doi.org/10.1021/acs.est.8b02709

Reinfelder, J. R., & Janssen, S. E. (2019). Tracking legacy mercury in the Hackensack River estuary using mercury stable isotopes. *Journal of Hazardous Materials*, *375*, 121–129. https://doi.org/10.1016/j.jhazmat.2019.04.074

Renedo, M., Amouroux, D., Pedrero, Z., Bustamante, P., & Cherel, Y. (2018). Identification of sources and bioaccumulation pathways of MeHg in subantarctic penguins: A stable isotopic investigation. *Scientific Reports*, *8*, 1–10. https://doi.org/10.1038/s41598-018-27079-9

Renedo, M., Bustamante, P., Cherel, Y., Pedrero, Z., Tessier, E., & Amouroux, D. (2020). A "seabird-eye" on mercury stable isotopes and cycling in the Southern Ocean. *Science of the Total Environment*, *742*. https://doi.org/10.1016/j.scitotenv.2020.140499

Renedo, M., Pedrero, Z., Amouroux, D., Cherel, Y., & Bustamante, P. (2021). Mercury isotopes of key tissues document mercury metabolic processes in seabirds. *Chemosphere*, *263*. https://doi.org/10.1016/j.chemosphere.2020.127777

Rodríguez-González, P., Epov, V. N., Bridou, R., Tessier, E., Guyoneaud, R., Monperrus, M., & Amouroux, D. (2009). Species-specific stable isotope fractionation of mercury

during Hg(II) methylation by an anaerobic bacteria (*Desulfobulbus propionicus*) under dark conditions. *Environmental Science and Technology*, *43*, 9183–9188. https://doi.org/10.1021/es902206j

Rothenberg, S. E., & Feng, X. (2012). Mercury cycling in a flooded rice paddy. *Journal of Geophysical Research-Biogeosciences*, *117*. https://doi.org/10.1029/2011JG001800

Rua-Ibarz, A., Bolea-Fernandez, E., Maage, A., Frantzen, S., Sanden, M., & Vanhaecke, F. (2019). Tracing Mercury Pollution along the Norwegian Coast via Elemental, Speciation, and Isotopic Analysis of Liver and Muscle Tissue of Deep-Water Marine Fish (*Brosme brosme*). *Environmental Science and Technology*, *53*, 1776–1785. https://doi.org/10.1021/acs.est.8b04706

Ruiz, X., Oro, D., Martinez-Vilalta, A., & Jover, L. (1996). Feeding ecology of Audouin's Gulls (*Larus audouinii*) in the Ebro Delta. *Colonial Waterbirds*, *19*, 68–74. https://doi.org/10.2307/1521947

Sánchez-Fortún, M., Ouled-Cheikh, J., Jover, C., García-Tarrasón, M., Carrasco, J. L., & Sanpera, C. (2020). Following up mercury pollution in the Ebro Delta (NE Spain): Audouin's gull fledglings as model organisms to elucidate anthropogenic impacts on the environment. *Environmental Pollution*, *266*, 1–9. https://doi.org/10.1016/j.envpol.2020.115232

Sanpera, C., Moreno, R., Ruiz, X., & Jover, L. (2007). Audouin's gull chicks as bioindicators of mercury pollution at different breeding locations in the western Mediterranean. *Marine Pollution Bulletin*, *54*(6), 691–696. https://doi.org/10.1016/j.marpolbul.2007.01.016

Schudel, G., Miserendino, R. A., Veiga, M. M., Velasquez-López, P. C., Lees, P. S. J., Winland-Gaetz, S., Davée Guimarães, J. R., & Bergquist, B. A. (2018). An investigation of mercury sources in the Puyango-Tumbes River: Using stable Hg isotopes to characterize transboundary Hg pollution. *Chemosphere*, *202*, 777–787. https://doi.org/10.1016/j.chemosphere.2018.03.081

Selin, N. E. (2009). Global Biogeochemical Cycling of Mercury: A Review. *Annual Review of Environment and Resources*, *34*(1), 43–63. https://doi.org/10.1146/annurev.environ.051308.084314

Senn, D. B., Chesney, E. J., Blum, J. D., Bank, M. S., Maage, A., & Shine, J. P. (2010). Stable isotope (N, C, Hg) study of methylmercury sources and trophic transfer in the northern Gulf of Mexico. *Environmental Science and Technology*, *44*, 1630–1637. https://doi.org/10.1021/es902361j

Sherman, L. S., & Blum, J. D. (2013). Mercury stable isotopes in sediments and largemouth bass from Florida lakes, USA. *Science of the Total Environment*, *448*, 163–175. https://doi.org/10.1016/j.scitotenv.2012.09.038

Suárez-Serrano, A., Alcaraz, C., Ibáñez, C., Trobajo, R., & Barata, C. (2010). *Procambarus clarkii* as a bioindicator of heavy metal pollution sources in the lower Ebro River and

997 Delta. *Ecotoxicology and Environmental Safety*, *73*, 280–286.
998 https://doi.org/10.1016/j.ecoenv.2009.11.001

999 Tsui, M. T.-K., Blum, J. D., & Kwon, S. Y. (2020). Review of stable mercury isotopes in
1000 ecology and biogeochemistry. *Science of the Total Environment*, *716*.
1001 https://doi.org/10.1016/j.scitotenv.2019.135386

1002 Ullrich, S. M., Tanton, T. W., & Abdrashitova, S. A. (2001). Mercury in the aquatic
1003 environment: A review of factors affecting methylation. *Critical Reviews in*
1004 *Environmental Science and Technology*, *31*(3), 241–293.
1005 https://doi.org/10.1080/20016491089226

1006 UNEP. (2019). *Global Mercury Assessment 2018*.
1007 http://www.unep.org/gc/gc22/Document/UNEP-GC22-INF3.pdf

1008 Washburn, S. J., Blum, J. D., Demers, J. D., Kurz, A. Y., & Landis, R. C. (2017). Isotopic
1009 Characterization of Mercury Downstream of Historic Industrial Contamination in the
1010 South River, Virginia. *Environmental Science and Technology*, *51*, 10965–10973.
1011 https://doi.org/10.1021/acs.est.7b02577

1012 Whitney, M. C., & Cristol, D. A. (2017). Impacts of sublethal mercury exposure on birds: A
1013 detailed review. *Reviews of Environmental Contamination and Toxicology*,
1014 *238*(December), 113–163. https://doi.org/10.1007/398_2017_4

1015 Wiederhold, J. G., Skyllberg, U., Drott, A., Jiskra, M., Jonsson, S., Björn, E., Bourdon, B., &
1016 Kretzschmar, R. (2015). Mercury isotope signatures in contaminated sediments as a
1017 tracer for local industrial pollution sources. *Environmental Science and Technology*, *49*,
1018 177–185. https://doi.org/10.1021/es5044358

1019 Wiener, J. G., Gilmour, C. C., & Krabbenhoft, D. P. (2003). Mercury Strategy for the Bay-
1020 Delta Ecosystem: A Unifying Framework for Science, Adaptive Management, and
1021 Ecological Restoration. http://science.calwater.ca.gov/library.shtml

1022 Yin, R., Feng, X., & Meng, B. (2013). Stable mercury isotope variation in rice plants (Oryza
1023 sativa L.) from the Wanshan mercury Mining District, SW China. *Environmental*
1024 *Science and Technology*, *47*, 2238–2245. https://doi.org/10.1021/es304302a

1025 Zheng, W., & Hintelmann, H. (2009). Mercury isotope fractionation during photoreduction in
1026 natural water is controlled by its Hg/DOC ratio. *Geochimica et Cosmochimica Acta*, *73*,
1027 6704–6715. https://doi.org/10.1016/j.gca.2009.08.016

1028
1029
1030
1031
1032
1033

1034

1035

1036 **Figures and Tables**

1037
1038

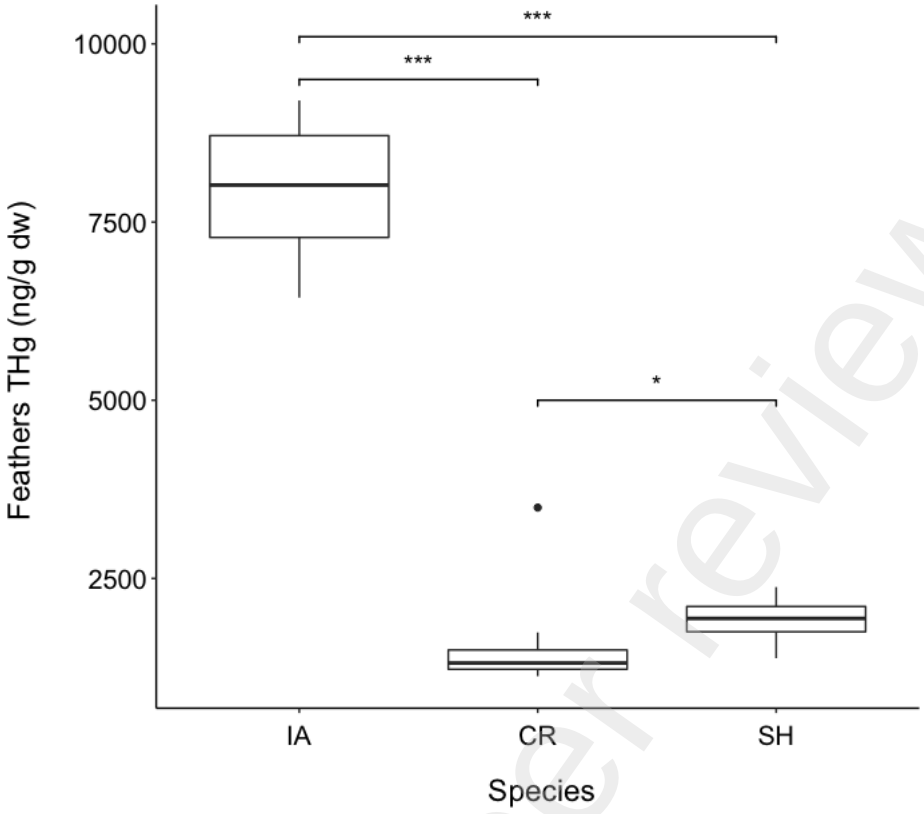

Figure 1. Boxplots for THg (ng/g dw) in feathers of Audouin's gulls (IA), black-headed gull (CR) and common tern (SH) fledglings from the Ebro Delta in 2017. Pairwise significant differences between species are represented above the boxplots (* $p<0.05$, ** $p<0.01$, *** $p<0.001$).

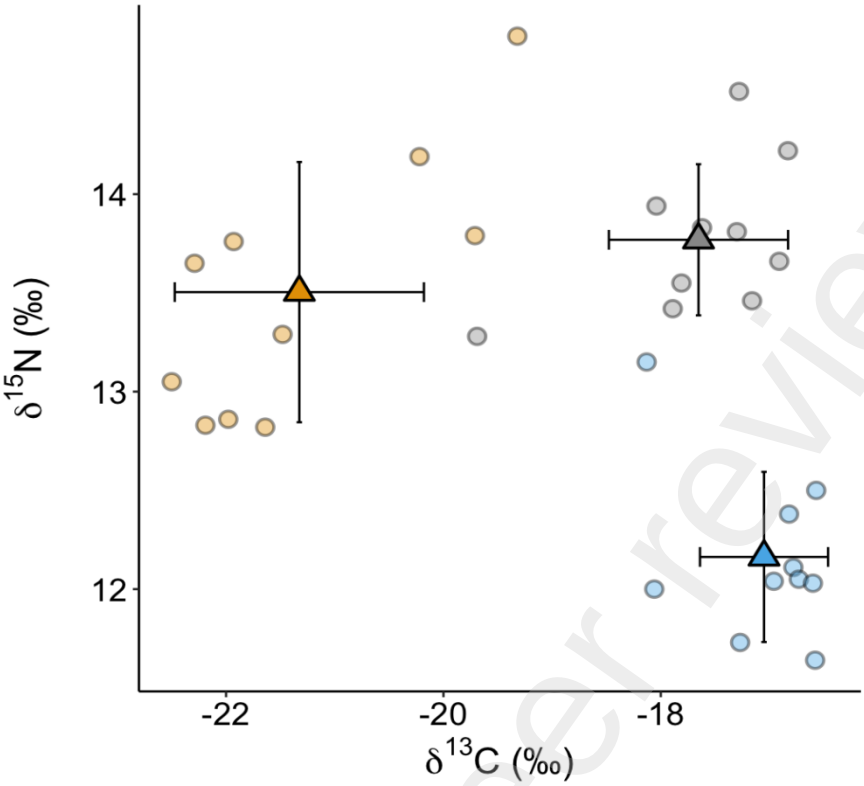

Figure 2. Biplot of $\delta^{15}N$ (‰) and $\delta^{13}C$ (‰) in feathers of Audouin's gulls (IA, in gray), black-headed gull (CR, in orange) and common tern (SH, in blue) fledglings from the Ebro Delta in 2017. Individual data are plotted as dots. Triangles and error bars represent mean ± SD.

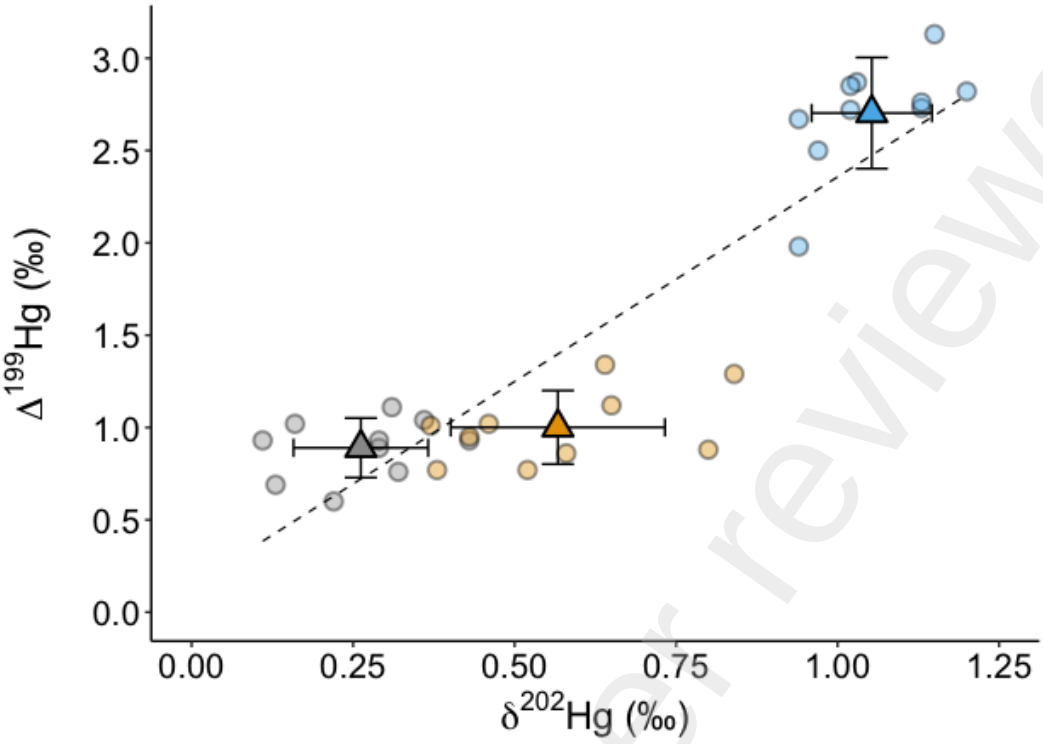

Figure 3. Biplot of MDF δ^{202}Hg (‰) and odd-MIF Δ^{199}Hg (‰) in feathers of Audouin's gulls (IA, in gray), black-headed gull (CR, in orange) and common tern (SH, in blue) fledglings from the Ebro Delta in 2017. Individual data are plotted as dots. Triangles and error bars represent mean ± SD. Dashed line represents linear regression between these variables for the three species: $y = 0.1407 + 2.2167x$; $R^2 = 0.7963$; $p < 0.0001$.

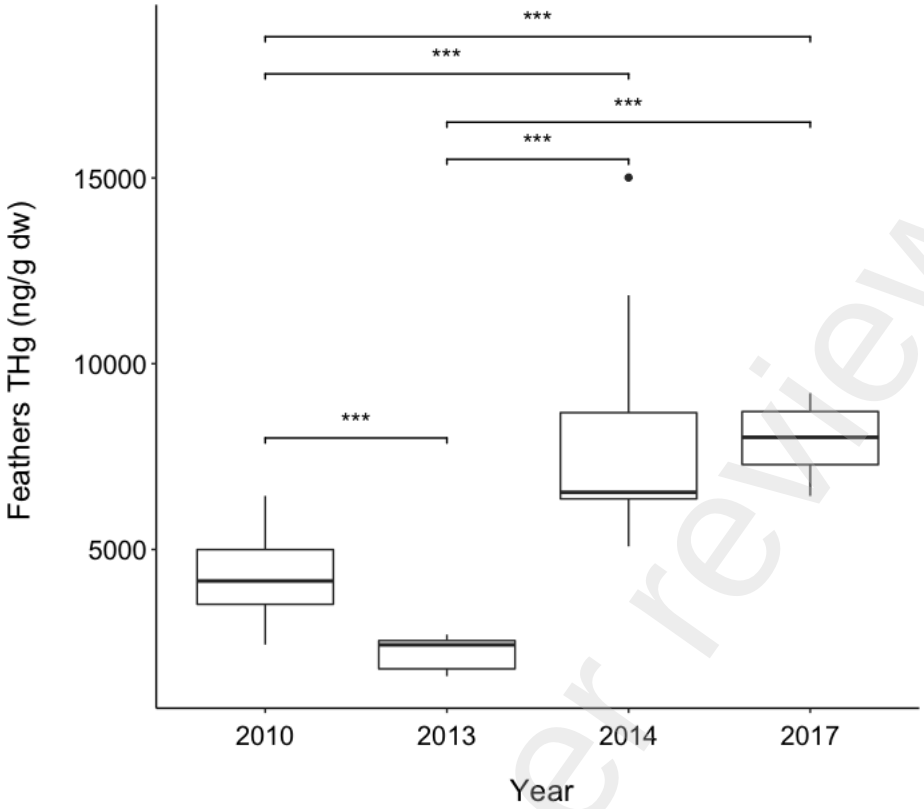

Figure 4. Boxplots for THg (ng/g dw) in feathers of fledglings Audouin's gulls (I. audouinii) from breeding seasons of 2010, 2013, 2014, 2017 (N = 10 individuals for each year) in the Ebro Delta breeding colony. Pairwise significant differences between years are represented above the boxplots (* $p<0.05$, ** $p<0.01$, *** $p<0.001$).

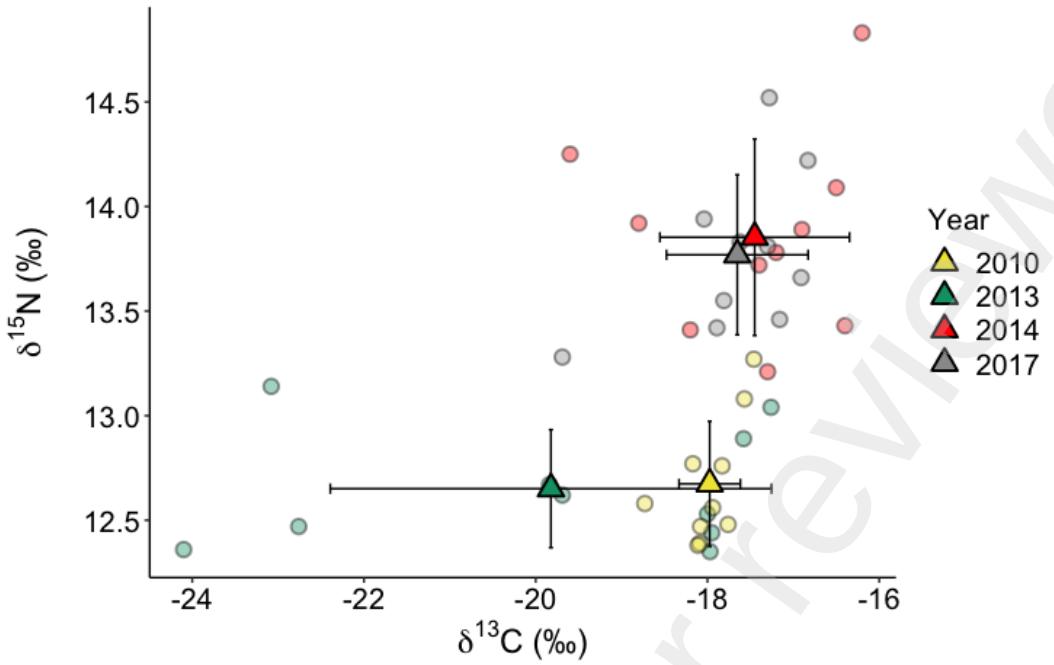

Figure 5. Biplot of $\delta^{15}N$ (‰) and $\delta^{13}C$ (‰) in feathers of Audouin's gulls (*I. audouinii*) fledglings from the Ebro Delta breeding colony in 2010, 2013, 2014 and 2017 (N = 10 individuals for each year). Individual data are plotted as dots. Triangles and error bars represent mean ± SD.

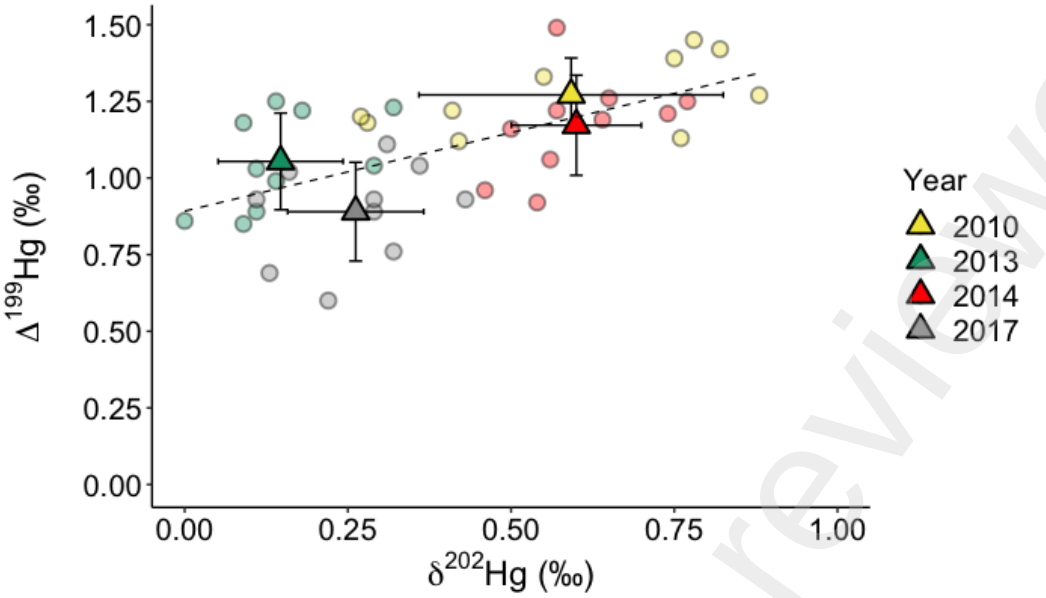

Figure 6. Biplot of MDF δ^{202}Hg (‰) and odd-MIF Δ^{199}Hg (‰) in feathers of Audouin's gulls (IA) fledglings from the Ebro Delta breeding colony in 2010, 2013, 2014 and 2017 (N = 10 individuals for each year). Individual data are plotted as dots. Triangles and error bars represent mean ± SD. Dashed line represents linear regression between these variables for all the years studied: $y = 0.8920 + 0.5115x$; $R^2 = 0.3611$; $p < 0.0001$.

Table 1. Summary statistics (mean, SD) for each of the parameters ($\delta^{15}N$, $\delta^{13}C$, THg, $\Delta^{199}Hg$, $\Delta^{201}Hg$) in fledglings feathers for each of the three species studied during the 2017 breeding season in the Ebro Delta. IA: *I. audouinii* (Audouin's gull), CR: *C. ridibundus* (black-headed gull), SH: *S. hirundo* (common tern).

	$\delta^{15}N$ (‰)				$\delta^{13}C$ (‰)				THg (ng/g dw)				$\Delta^{199}Hg$ (‰)				$\Delta^{201}Hg$ (‰)				$\delta^{202}Hg$ (‰)			
Species	Mean	SD	Max	Min	Mean	SD	Max	Min	Mean	SD	Max	Min	Mean	SD	Max	Min	Mean	SD	Max	Min	Mean	SD	Max	Min
IA	13.77	0.38	14.52	13.28	-17.65	0.82	-16.83	-19.69	7982.97	951.94	9205.55	6439.79	0.89	0.16	1.11	0.60	0.68	0.14	0.85	0.38	0.26	0.10	0.43	0.11
CR	13.50	0.66	14.80	12.82	-21.33	1.15	-19.32	-22.50	1555.94	704.45	3494.11	1128.31	1.00	0.20	1.34	0.77	0.78	0.19	1.13	0.54	0.57	0.17	0.84	0.37
SH	12.16	0.43	13.15	11.64	-17.05	0.59	-16.57	-18.13	1916.14	284.04	2379.45	1381.47	2.70	0.30	3.13	1.98	2.23	0.26	2.61	1.62	1.05	0.09	1.20	0.94

Table 2. Pearson's correlation tests between each of the mercury isotopic tracers ($\delta^{202}Hg$, $\Delta^{199}Hg$ and $\Delta^{201}Hg$) and THg, $\delta^{13}C$, and $\delta^{15}N$ in fledglings feathers for each of the three species studied during the 2017 breeding season in the Ebro Delta. IA: *I. audouinii* (Audouin's gull), CR: *C. ridibundus* (black-headed gull), SH: *S. hirundo* (common tern). Significant correlations are highlighted in bold.

		Audouin's gull (IA)			Black-headed gull (CR)			Common tern (SH)		
		$\delta^{202}Hg$	$\Delta^{199}Hg$	$\Delta^{201}Hg$	$\delta^{202}Hg$	$\Delta^{199}Hg$	$\Delta^{201}Hg$	$\delta^{202}Hg$	$\Delta^{199}Hg$	$\Delta^{201}Hg$
THg	r	-0.21	-0.41	-0.34	0.05	0.19	0.17	-0.51	**-0.85**	**-0.83**
	p-value	0.56	0.23	0.34	0.88	0.60	0.63	0.13	**0.002**	**0.002**
$\delta^{13}C$	r	-0.14	**0.66**	**0.72**	-0.03	0.56	**0.65**	0.07	0.44	0.44
	p-value	0.70	**0.04**	**0.02**	0.94	0.09	**0.04**	0.86	0.21	0.20
$\delta^{15}N$	r	-0.50	-0.09	-0.03	0.03	0.48	0.52	0.18	-0.09	-0.16
	p-value	0.14	0.80	0.92	0.93	0.16	0.12	0.63	0.80	0.65

Table 3. Summary statistics (mean, SD, max and min) for each of the parameters ($\delta^{15}N$, $\delta^{13}C$, THg, $\Delta^{199}Hg$, $\Delta^{201}Hg$ and $\delta^{202}Hg$) in fledglings' feathers for each of the years studied (2010, 2013, 2014 and 2017) on the Audouin's gull (*I. audouinii*) breeding colony in the Ebro Delta.

	$\delta^{15}N$ (‰)				$\delta^{13}C$ (‰)				THg (ng/g dw)				$\Delta^{199}Hg$ (‰)				$\Delta^{201}Hg$ (‰)				$\delta^{202}Hg$ (‰)			
Year	Mean	SD	Max	Min	Mean	SD	Max	Min	Mean	SD	Max	Min	Mean	SD	Max	Min	Mean	SD	Max	Min	Mean	SD	Max	Min
2010	12.67	0.30	13.27	12.38	-17.97	0.36	-17.46	-18.73	4288.55	1260.41	6441.93	2438.68	1.27	0.12	1.45	1.12	1.02	0.11	1.16	0.89	0.59	0.23	0.88	0.27
2013	12.65	0.28	13.14	12.35	-19.82	2.57	-17.26	-24.10	2227.59	443.56	2710.85	1588.99	1.05	0.16	1.25	0.85	0.85	0.12	1.00	0.67	0.15	0.10	0.32	0.00
2014	13.85	0.47	14.83	13.21	-17.45	1.10	-16.20	-19.60	8032.03	3119.42	15009.73	5084.04	1.17	0.16	1.49	0.92	0.96	0.25	1.57	0.63	0.60	0.10	0.77	0.46
2017	13.77	0.38	14.52	13.28	-17.65	0.82	-16.83	-19.69	7982.97	951.94	9205.55	6439.79	0.89	0.16	1.11	0.60	0.68	0.14	0.85	0.38	0.26	0.10	0.43	0.11

Table 4. Pearson's correlation tests between each of the mercury isotopic tracers ($\delta^{202}Hg$, $\Delta^{199}Hg$ and $\Delta^{201}Hg$) and THg, $\delta^{13}C$, and $\delta^{15}N$ in fledglings' feathers for each of the years studied (2010, 2013, 2014 and 2017) and for all the years together on the Audouin's gull (*I. audouinii*) breeding colony in the Ebro Delta. Significant correlations are highlighted in bold.

		2010			2013			2014			2017			All Years		
		$\delta^{202}Hg$	$\Delta^{199}Hg$	$\Delta^{201}Hg$	$\delta^{202}Hg$	$\Delta^{199}Hg$	$\Delta^{201}Hg$	$\delta^{202}Hg$	$\Delta^{199}Hg$	$\Delta^{201}Hg$	$\delta^{202}Hg$	$\Delta^{199}Hg$	$\Delta^{201}Hg$	$\delta^{202}Hg$	$\Delta^{199}Hg$	$\Delta^{201}Hg$
THg	r	0.49	0.38	0.28	-0.32	-0.52	-0.47	-0.07	0.46	0.49	-0.18	-0.41	-0.33	0.29	-0.09	-0.02
	p-value	0.15	0.28	0.43	0.37	0.13	0.17	0.84	0.19	0.15	0.61	0.24	0.33	0.07	0.57	0.91
$\delta^{13}C$	r	-0.07	-0.38	-0.44	-0.35	-0.39	-0.37	0.46	0.47	0.22	-0.14	**0.66**	**0.72**	0.29	0.04	0.03
	p-value	0.84	0.28	0.20	0.32	0.26	0.29	0.18	0.17	0.54	0.70	**0.04**	**0.02**	0.07	0.83	0.85
$\delta^{15}N$	r	0.11	-0.29	-0.49	0.17	-0.41	-0.37	0.45	-0.14	-0.38	-0.50	-0.09	-0.03	0.15	**-0.32**	**-0.34**
	p-value	0.77	0.42	0.15	0.63	0.24	0.29	0.20	0.71	0.28	0.14	0.80	0.92	0.33	**0.04**	**0.031**